



## GCM Mapping Salten

Report number 19-12-2017, December 2017





## Indholdsfortegnelse

<b>1. Project information .....</b>	<b>2</b>
<b>2. DUALEM-421s .....</b>	<b>3</b>
2.1 Setup and functionality .....	3
2.2 Sensitivity distribution .....	4
2.3 Disadvantages.....	6
2.4 The resistivity of various soil types .....	7
<b>3. Data collection .....</b>	<b>9</b>
3.1 Data drift quality control.....	9
<b>4. Processing .....</b>	<b>11</b>
<b>5. Inversion .....</b>	<b>13</b>
5.1 The SCI-method.....	13
5.2 Depth of Investigation .....	15
5.3 Mean-resistivity maps .....	16
<b>6. Results .....</b>	<b>18</b>
6.1 Quality control maps .....	19
Model Location and GCM Lines .....	19
Data Residual .....	19
Depth of Investigation (DOI) .....	19
6.2 Mean Resistivity maps.....	20
6.3 Profiles .....	21



## 1. PROJECT INFORMATION

The aim of the project "Afvanding, klimatilpasning og fremtidens vandløbsregulering" is to secure farmers higher and more stable yield on fields, which, today, are facing issues due to excess water. This will be done on the basis of an example from Salten (Løvenholt Gods), where we will investigate causes and solutions to poor draining/dewatering of wet spots on the fields. This is done together with farmers and consultants.

In this context, HGG, AU have mapped a 26 hectare big area close to Salten (Løvenholt gods) by means of geophysical methods. The aim of the mapping was to map the shallow soil layers (upper 5-8 m) and in depth (upper 30 m). This was done with a 10 m line distance with the GCM (DualEM) and tTEM (towTEM) methods. This report describes the data collection, data processing, data inversion and results.

GCM mapping – Salten	
Contact person	<b>HGG, Aarhus University, Denmark</b> <i>Jesper B. Pedersen</i> <b>SEGES, Denmark</b> <i>Rikke Laursen</i>
Locality	Salten, Denmark
Field period	The 7th of October, 2017
Line spacing	10 m
Total number of measurements	14508
Report	Prepared by: <i>Jesper B. Pedersen, Pradip Maurya, Rune Kraghede &amp; Kim Engebretsen</i>

Table 1. Project information



## 2. DUALEM-421S

### 2.1 Setup and functionality

The DUALEM-421S is a Ground Conductivity Meter (GCM) instrument using electromagnetic induction to estimate the electrical resistivity distribution in the subsurface.

The instrument consists of a horizontal transmitter coil mounted at one end of a 4-m long tube. Within the tube, three pairs of receiver coils are mounted at a distance of respectively 1, 2, and 4 m from the transmitter coil. In each pair of receiver coils one coil is placed horizontally (HCP-configuration) and the other vertically (PRP-configuration). See figure 1 and 2 for a sketch of the DUALEM-421S instrument. The DUALEM-421S instrument is pulled behind an ATV at a distance of approximately 4 m where it will not influence the measurements (see Figure 3).



Figure 1. Sketch of the transmitter (Tx) and receiver (Rx) coils in a DUALEM-421S system. For the HCP-configuration the Rx-coil is placed on the same horizontal plane as the transmitter coil. For the PRP-configuration the Rx-coil is perpendicular to the Tx-coil and centered around the Tx-coil's horizontal plane.



Figure 2. Sketch of the DUALEM-421s instrument. The transmitter coil (Tx) is placed at one end of the tube and the 3 receiver coil pairs (Rx) at a distance of 1, 2, and 4 m from the transmitter coil.



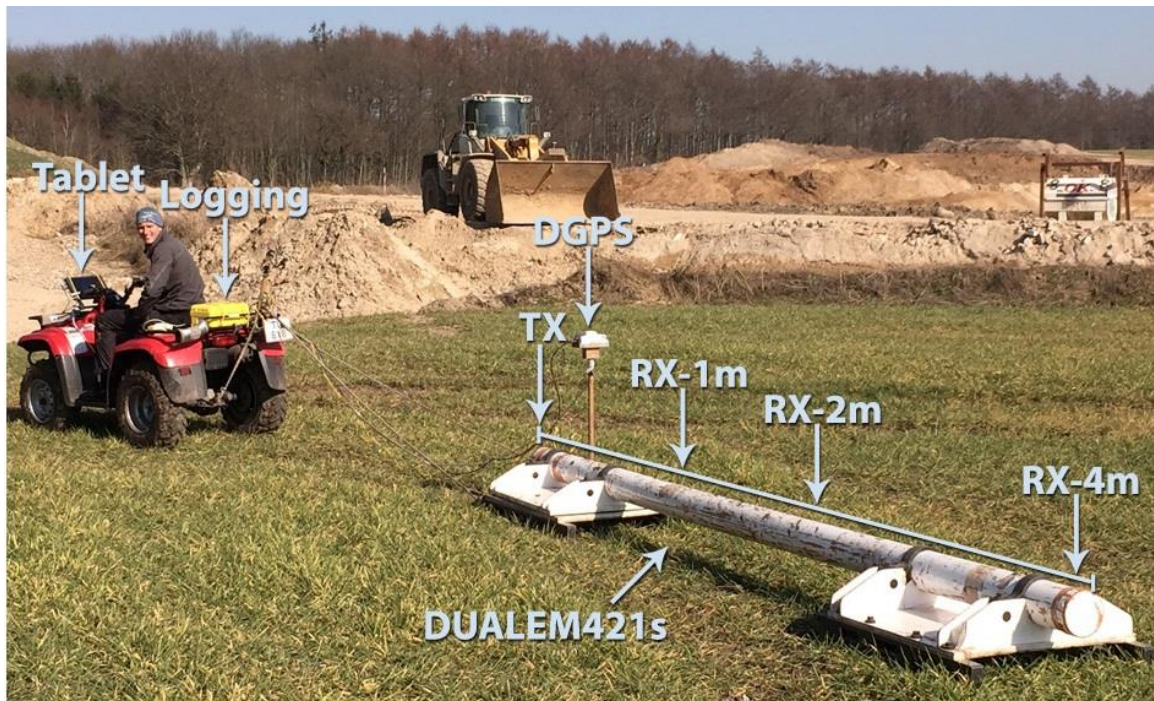


Figure 3. Field setup. The DUALEM-421s instrument is pulled by an ATV. The instrument is equipped with a GPS for accurate positioning of the measurements.

An alternating current is sent through the transmitter coil, forming a primary magnetic field in the ground, alternating at the same frequency as the current.

Variations in the magnetic field induce a varying electrical field in the ground, which again forms a varying secondary magnetic field that can be measured by the receiver coils. This secondary magnetic field contains information about the ground's electrical properties.

The DUALEM-421s is a frequency domain system that continuously transmits a primary field with a frequency of 9 kHz. The receiver coils measure the secondary field's amplitude and phase. Amplitude and phase are measured in relation to the primary field.

## 2.2 Sensitivity distribution

The sensitivity of the subsurface layers at various depths depends on the resistivity of the layers (the geology), the choice of frequency, the distance between the transmitter and the receiver coils, and the orientation of the coils in relation to each other. For the DUALEM-421s-system the frequency and the geometry of the coils are



fixed, but since there are three pairs of receiver coils, a total of 6 independent configurations is achieved. For each of these 6 configurations both amplitude and phase are measured, but the phase is traditionally difficult to calibrate on these instruments and we have chosen not to use it in the interpretation. Thus, we get 6 data points per measurement. These 6 data points contain information about different parts of the ground, since they have different vertical sensitivity distributions. Generally, the HCP-configurations penetrate deeper than the PRP-configurations, and configurations with a longer coil distance penetrate deeper than configurations with a shorter coil distance.

For a HCP-configuration the 1D sensitivity function is described as:

$$S^{HCP}(z) = \frac{4z}{(1 + 4z^2)^{\frac{3}{2}}}$$

For PRP the 1D sensitivity function is expressed by:

$$S^{PRP}(z) = \frac{2}{(1 + 4z^2)^{\frac{3}{2}}}$$

For both equations  $z$  is a normalized depth,  $z = d/r$ , where  $d$  is depth and  $r$  is the distance between transmitter and receiver coils. The sensitivity functions for the 6 configurations is shown in Figure 4, where the left plot shows the above equations (normalized with the total sensitivity) and the right plot shows the cumulated sensitivities.

From the sensitivity functions, it can be seen that the PRP-configurations contain the most information at the surface whereas the HCP configurations have little sensitivity at the top with a distinct maximum somewhere below the surface.

In the summated sensitivity functions in Figure 4 an estimate of the focus depth is shown with a circle. The focus depth is indicated at the depth at which 50% of the sensitivity is reached. For the HCP configuration of 1 m the focus depth is ca. 0.87 m (1.73 m for a 2-m coil distance and 3.5 m for a 4-m coil distance). For the PRP configuration with a coil distance of 1.1 m the focus depth is found at ca. 0.32 m and correspondingly at 0.61 m with a coil distance of



2.1 m, and at 1.2 m for a PRP-configuration with a coil distance of 4.1 m. Hence, the HCP configurations have a deeper sensitivity-distribution than the PRP-configurations.

These indicated maximum sensitivities and focus depths are based on the assumption that the equipment measures from the ground surface. As this GCM equipment measures from 30 cm over the ground surface the values will be slightly less as some of the sensitivity is lost in the air.

The GCM-system is mounted on a sled, which is pulled by an ATV, thus achieving a fast and navigable system that can map many km per day.

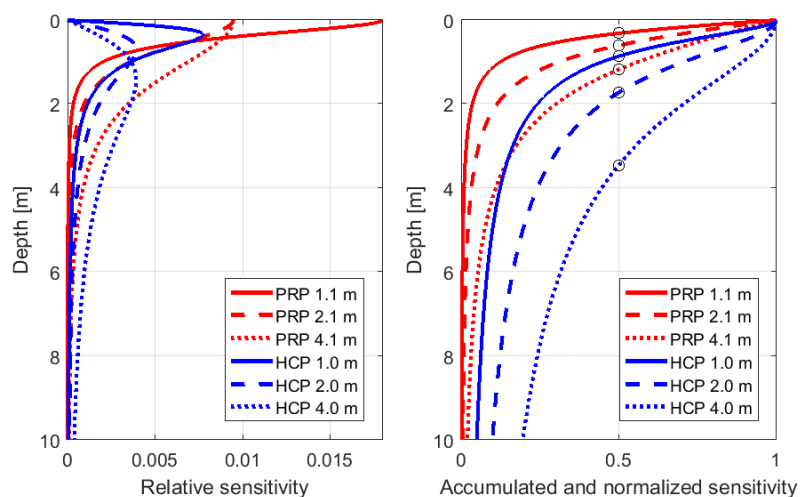


Figure 4. **Left:** Sensitivity function for HCP (blue curves), og PRP (red curves). **Right:** The integrated sensitivity function for HCP (blue curves) and PRP (red curves).

### 2.3 Disadvantages

Like all other electromagnetic methods, the GCM method is influenced by external sources of noise like fences, metal pipes in the ground, power lines etc. and it is necessary to measure somewhat away from these sources for them not to influence the measurements. The larger the source of noise the further away you need to be.

The DUALEM-421S instrument has 6 receiver coils and thus 6 data points are achieved for each measurement. Ideally, with 6 data points you can interpret 6 parameters – for instance the resistivity of 6 layers with fixed layer boundaries. In practice, more than 6



layers are used in the interpretation, and the layers are connected by lateral and vertical constraints in order to have a robust solution which at the same time complies with the expected geological variations. The relatively few data points and expected penetration depths must be taken into account when evaluating the results of the inversion.

## 2.4 The resistivity of various soil types

With the GCM method the resistivity in the ground can be measured to a depth of approximately 7 m. The measured resistivity depends on several factors like lithology, water content and the ion content in the water. Figure 5 shows the relative resistivity of different Danish lithologies in and the relation to water quality. Figure 6 shows the values of typical resistivities of Danish lithologies. Due to the chemical composition clay deposits are characterized by having a low resistivity while layers of sand or gravel have a high resistivity

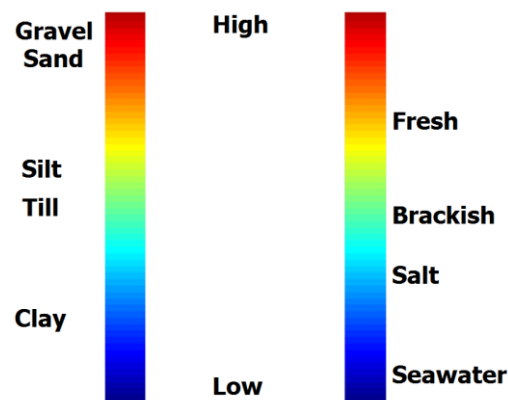


Figure 5. Relative resistivity of various lithologies and the relation to water quality.

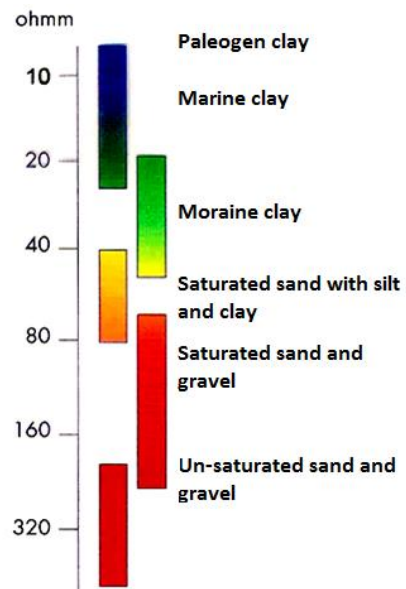


Figure 6. The resistivity of different Danish lithologies.





### 3. DATA COLLECTION

The data collection was carried out the 7<sup>th</sup> of October, 2017. The survey area was mapped with 10 m line spacing and 14.508 measurements were collected during the mapping campaign (see *Figure 7*).

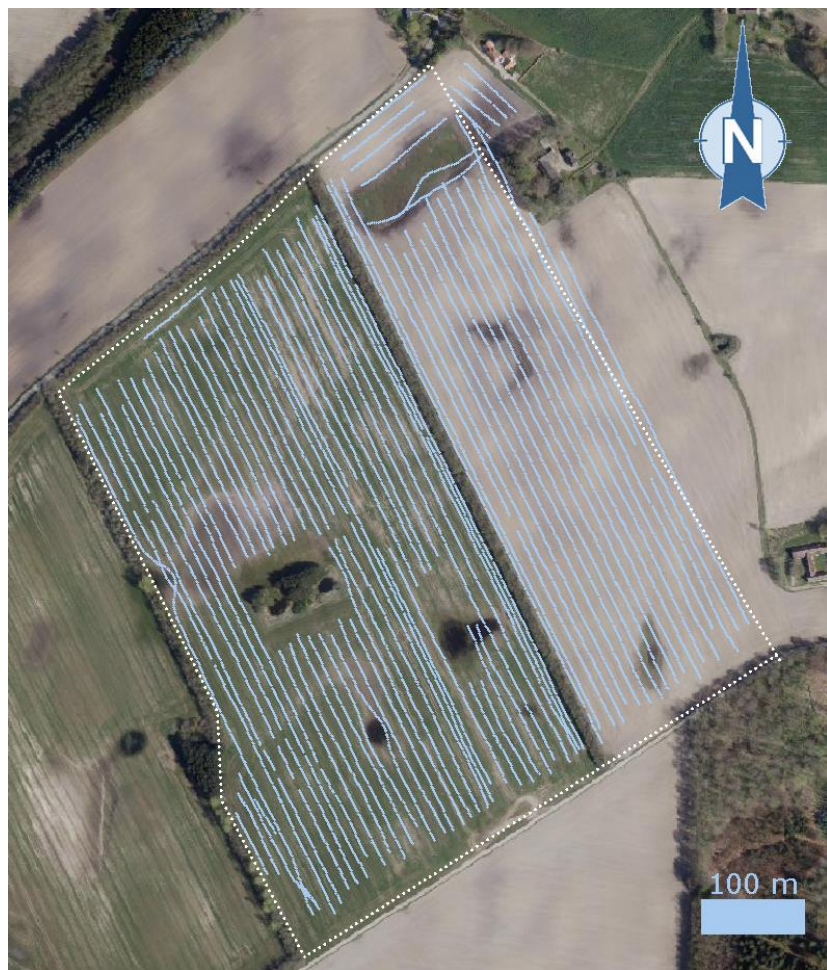


*Figure 7. Map of measurements. Measurements are shown with blue points.*

#### 3.1 Data drift quality control

With the DUALEM421 system the geometry, i.e. the distances between the transmitter coils and receiver coils, are presumed constant when interpreting the measured data. Potentially, changes in the presumed system geometry can result in faulty interpretations, since the calculated resistivity in the subsurface can be either too high or too low. This is called data drift. Changes in the system



geometry are rarely seen, but can take place in case of for instance significant temperature changes in the instrument. High temperatures may make the receiver coils expand, which causes data drift, as the presumed system geometry is changed.

Another cause for data drift can be mapping in a rough terrain. If the instrument is handled roughly by bumping through rough terrain it can influence the internal placing of the transmitter and receiver coils.

In order to verify that data are not influenced by data drift a quality control point and/or line is established for each mapping area. The quality control point and line is GPS referenced. The point and/or line is measured twice with the GCM instrument, once before and once after the data collection on a daily basis during the survey period. The result of the measurements should be close to identical for all 6 receiver coil configurations. Should this not be the case a data shift can be applied to the data channels influenced by drift. No data drift was observed for the Salten survey.



## 4. PROCESSING

The processing of the GCM data is carried out in the Aarhus Workbench. The objective of the processing is to make the data ready for inversion and interpretation. Only the amplitude data, not the phase, from the measurements are used. Generally, the data quality is good and only negative and noise influenced data have been removed in the processing. Negative and noise influenced data are mainly seen at the end of a line where instruments has been turned to start the next line. Further, the data have been averaged with a running mean filter. We achieve a raw measurement approximately every 30 cm, which after the filtering results in a measurement for every 2 m.

The uncertainty of the data has been estimated. This is done to assign more uncertainty to data measured on higher resistivities where the signal level is the lower. Typically, the noise from a GCM instrument is additive to the measured response, which is usually indicated in ppm (parts per million). From the instrument software, the measurements are indicated as apparent resistivity ( $\rho_a$ ):

$$\sigma_a = \frac{1}{\rho_a} = \frac{4}{\omega \mu_0 s^2} \text{ppm} \cdot 10^{-6}$$

where  $s$  is the coil distance,  $\omega = 2\pi f$  is the angular frequency for the frequency,  $f$  [Hz], and  $\mu_0 = 4\pi \cdot 10^{-7}$ . In order to calculate the uncertainty data values for individual data point are converted from apparent resistivity to ppm by rewriting the equation above:

$$\text{ppm}_{\text{m\AA}lt} = \frac{1,974 \cdot f \cdot s^2}{\rho_a}$$

Table 1 shows the added absolute uncertainty for each receiver coil configuration 1 ppm. A 3% uniform uncertainty has been added on top of that.

Receiver coil configuration	PRP1	HCP1	PRP2	HCP2	PRP4	HCP4
Uncertainty [ppm]	2.44	4.30	17.99	20.43	72.96	43.55

Table 1. Absolute uncertainty for each receiver coil configuration.

The total relative data uncertainty,  $\Delta\rho_a$  for the individual data point is then:





$$\Delta_{\rho_a} = \sqrt{0,03^2 + \left(\frac{ppm_{unc}}{ppm_{målt}}\right)^2}$$



## 5. INVERSION

Inversion and evaluation of inversion results are performed with Aarhus Workbench, which uses the inversion code AarhusInv, both have been developed by the HydroGeophysics Group, Aarhus University.

The data are inverted with a 1D SCI model setup. The settings for the inversion are shown in Table 2.

		Value
Software	Aarhus Workbench Version	5.5.0.0
Start model	Number of layers	12
	Start resistivity [ $\Omega\text{m}$ ]	40
	Layer thickness first layer [m]	0.2
	Depth to last layer [m]	10
	Distribution of layer thickness	Logarithmically rising with depth
SCI constraints	Horizontal constraints on resistivities [factor]	1.6
	Reference distance [m]	2
	GCM height above ground	30 cm
	Vertical constraints on resistivities [factor]	4.0
	Prior, thickness	Fixed
	Prior, resistivities	None
	Number of SCI cells	1

Table 2. Inversion settings, smooth SCI setup.

### 5.1 The SCI-method

The SCI inversion method (Spatially Constrained Inversion) uses constraint between the 1D model along as well as across the measurement lines (Figure 8). The inversion is a nonlinear dampened least squares method where the instrument's transfer function is fully modelled to its known extent (filters, wave forms, geometry).

The instrument height is as a model parameter in the inversion and is routinely carried out for airborne measurements. For the GCM measurements we do not have actual measurements of the instrument height and thus this is fixed in the inversion.

The model parameters in the models of the SCI interpretation is tied to a distance dependent variance. The constraints between the measurements are tied together form Delaunay triangles (Figure 9), by which each measurement is tied to its 'best neighbors'. Delaunay triangulation always connect neighboring lines with the



primary function of breaking down the line orientation in the data. In this way, we can avoid matters where the inversion results are influenced by data measured in lines. By tying together the model parameters, we achieve a better resolution of resistivities and layer borders than by performing an inversion of each individual measurement.

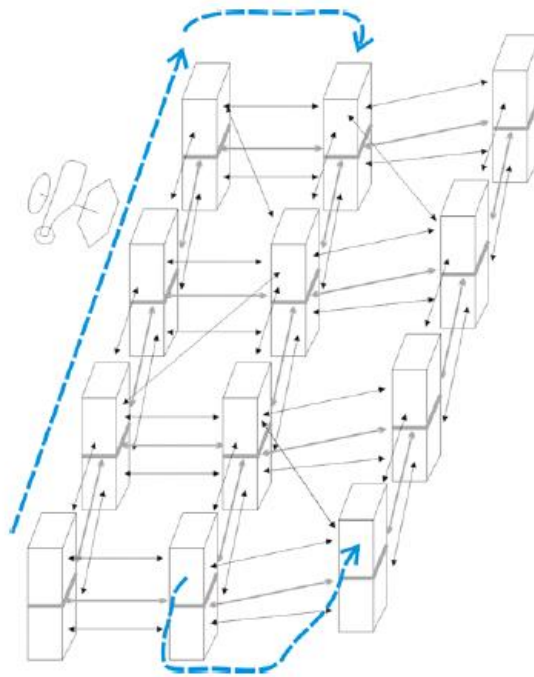


*Figure 8. Schematic concept of an SCI inversion. In the inversion constraints are used along and across the driving lines.*

An SCI inversion can be used for a few layer model (3-6 layers) with free parameters as well as for a many layer model (10-30 layers) with fixed thickness, but free resistivities. For a many layer model, vertical constraints are used between the layers in order to achieve a more stable inversion. Here only many layer models are used.

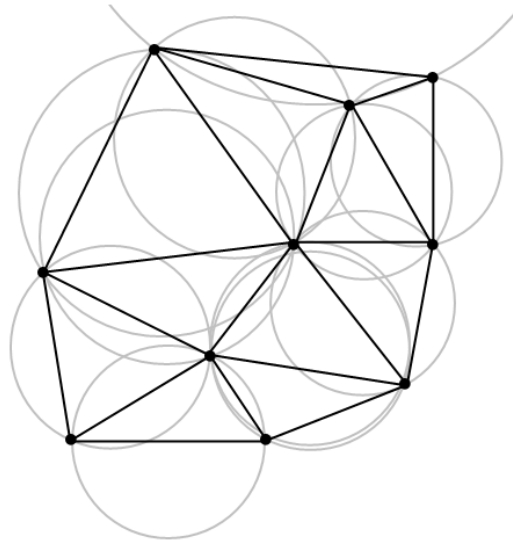


Figure 9. Example of Delaunay triangulation of points on one plane.

## 5.2 Depth of Investigation

For each model a conservative and standard DOI (Depth Of Investigation) is calculated, where system parameters, all data points and data uncertainties are considered. The model parts lying above the conservative DOI can be presumed to be well-founded in the data. Estimated values lying below the standard DOI should not be used for the interpretation of data, and values between the conservative and standard DOI can be used with caution.

The DOI is calculated from the calculated sensitivity matrix (Jacobian) from the final model. It is only data based and thus a priori information and constraints do not influence the calculation of the DOI. An example of DOI is shown in Figure 11 to the left where the sensitivity function is plotted based on a 3-layer model from a TEM sounding. The function is calculated from the sensitivity matrix and shows a higher sensitivity in layers with low resistivities (layer 1 and 3).

If you plot the integrated sensitivity function from the depth you will get the plot shown to the right in Figure 11. In this example, a DOI limit has been set at a cumulated sensitivity of 0,8. This means that there is not enough sensitivity below this depth for the information to be used for interpretation.

Conservative and standard DOI indicated in the Workbench are set at respectively 0,6 and 1,2. For GCM interpretations we use the standard DOI value as the limit.

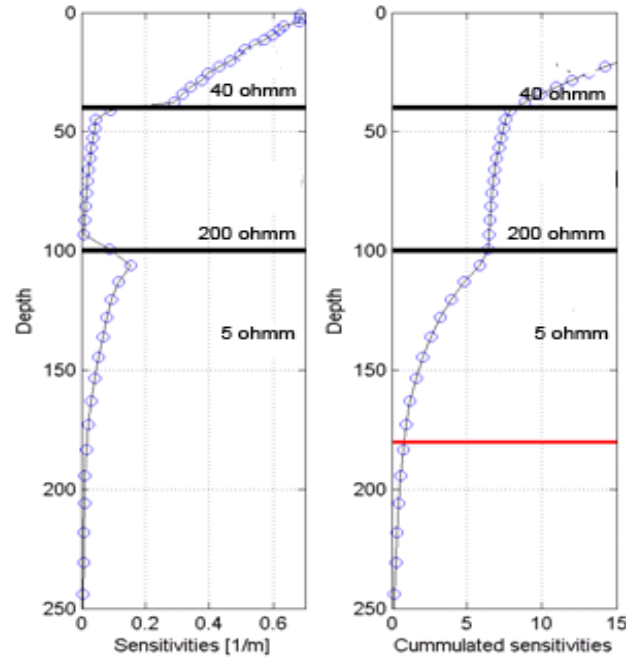


Figure 10. Calculated sensitivities for a 3-layer model performed with TEM. Left: the sensitivity function where the sensitivity is higher for the layers with low resistivities. Right: the integrated sensitivity function. De red line indicates DOI with a sensitivity of 0,8.

### 5.3 Mean-resistivity maps

The results from the inversion are 1D models describing depth intervals (layers) and the resistivities of each depth interval. For visualizing the results a mean-resistivity map is made, showing a calculated mean-resistivity of a given depth interval. The calculations for each model are shown in Figure 11, where  $[A,B]$  is the desired depth interval,  $[d_0:d_3]$  is the depth to the layer border, and  $[\rho_1;\rho_4]$  are the resistivities for each layer. Here the desired depth interval is split into 3 thicknesses  $[\Delta t_1: \Delta t_3]$  and the mean-resistivities are calculated by:

$$\rho_{vertical} = \frac{\rho_1 \cdot \Delta t_1 + \rho_2 \cdot \Delta t_2 + \rho_3 \cdot \Delta t_3}{\Delta t_1 + \Delta t_2 + \Delta t_3}$$

A general expression of the mean-resistivity in a given depth interval is:

$$\overline{\rho_{vertical}} = \frac{\sum_{i=1}^n \rho_i \cdot \Delta t_i}{\sum_{i=1}^n \Delta t_i}$$



$i$  goes from 1 to the number of thicknesses in the give depth interval. This calculated mean-resistivity equals the average resistivity if a current is sent vertically through the interval.

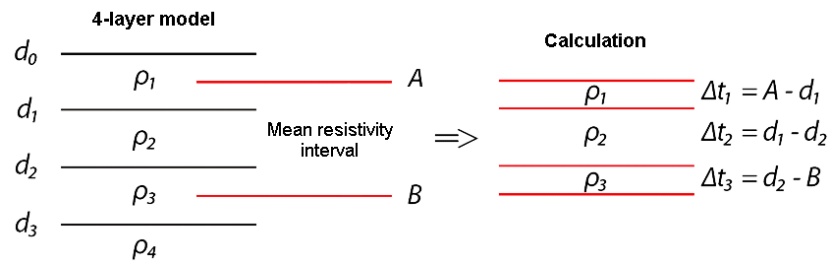


Figure 11. Calculation of mean-resistivity for the depth interval  $[A,B]$ .

The mean-resistivity can also be calculated when the current is sent horizontally through the depth interval. This is called the horizontal mean-resistivity. It is calculated as the reciprocal mean conductivity  $\sigma_{mean}$  and is given by:

$$\rho_{horizontal} = \frac{1}{\sigma_{mean}} = \left[ \frac{\sum_{i=1}^n \left( \frac{1}{\rho_i} \right) \cdot \Delta t_i}{\sum_{i=1}^n \Delta t_i} \right]^{-1}$$

Usually, the difference between these two calculated mean-resistivities is small, but the horizontal mean-resistivity emphasizes the lower resistivities, which are often those of most interest.

For the GCM data the mean-resistivity maps are calculated with a horizontal mean-resistivity. Kriging has been used for interpolation with a search radius of 10 m.



## 6. RESULTS

In the following, the result of the mapping is shown as quality control maps, mean-resistivity maps and profiles.

A total of 6 boreholes, drilled to 1,5 m depth, has also been carried out in the area by Casper Szilas from GPS agro. These boreholes have been plotted on top of the profiles. For a detailed description the boreholes and their good agreement with the GCM/EMI and tTEM data we refer the user to the paper "Notat vedr. profi-lundersøgelser ved Løvenholt" by Casper Szilas, GPS Agro. In the paper there is a detailed comparison of the EMI results and the boreholes.

To summarize the results, the geophysical mapping reveals that on the eastern field we see very high resistivity's almost at ground surface, which corresponds well with meltwater sand, which has a high resistivity of more than 100 ohm-m. In some areas it is so resistive that we don't get a signal with the tTEM method and hence the data had to be discarded. In these areas we still have GCM data. From 10 m depth and to more than 70 meters depth the tTEM results reveal a large meltwater sand aquifer. This aquifer extends below both the western and eastern field.

The shallow geology is much more complex on the western field. There are large variations in the area from resistive strongly sandy deposits (meltwater sand) to conductive clay/organic matter rich deposits (meltwater clay). This is especially evident in the mean-resistivity maps based on the GCM results. These are made in 0.5 to 1 meter slices from 0-5 meters depth. The local lows in the fields have been superimposed on the mean-resistivity maps as black contours. It is very clear from these maps that there is a strong correlation between the areas where there is standing water on the fields and the spots where there is a local low and meltwater clay in the upper 1-5 meters. The thick meltwater clay sequence acts as a barrier so the water can't infiltrate.



## 6.1 Quality control maps

In the following quality control maps are shown.

### Model Location and GCM Lines

This map shows the actual GCM lines. Grey dots mark where data are disregarded due to line turns or coupling. Black dots mark where data is kept and inverted to a resistivity model.

A relatively small amount of data is disregarded due to turns with the instrument, where the equipment is too close to the ATV in order to get reliable measurements.

### Data Residual

The data residual tells how well the obtained resistivity models explain the recorded data (how well the data is fitted). The data residual values are normalized with the data standard deviation, so a data residual below one corresponds to a fit within one standard deviation.

The data residual map is for the smooth inversion result. Some areas have relatively high data residual values ( $>2$ ), this is primarily due to noise data, which again is associated to low signal ground responses (resistive ground). In general, the data residuals are as expected for this type of environment and geological setting.

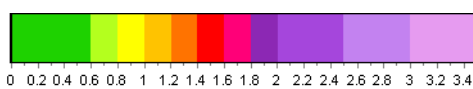
### Depth of Investigation (DOI)

This map shows the DOI estimates for the smooth model inversion result. DOI maps in depths are included in the appendix.

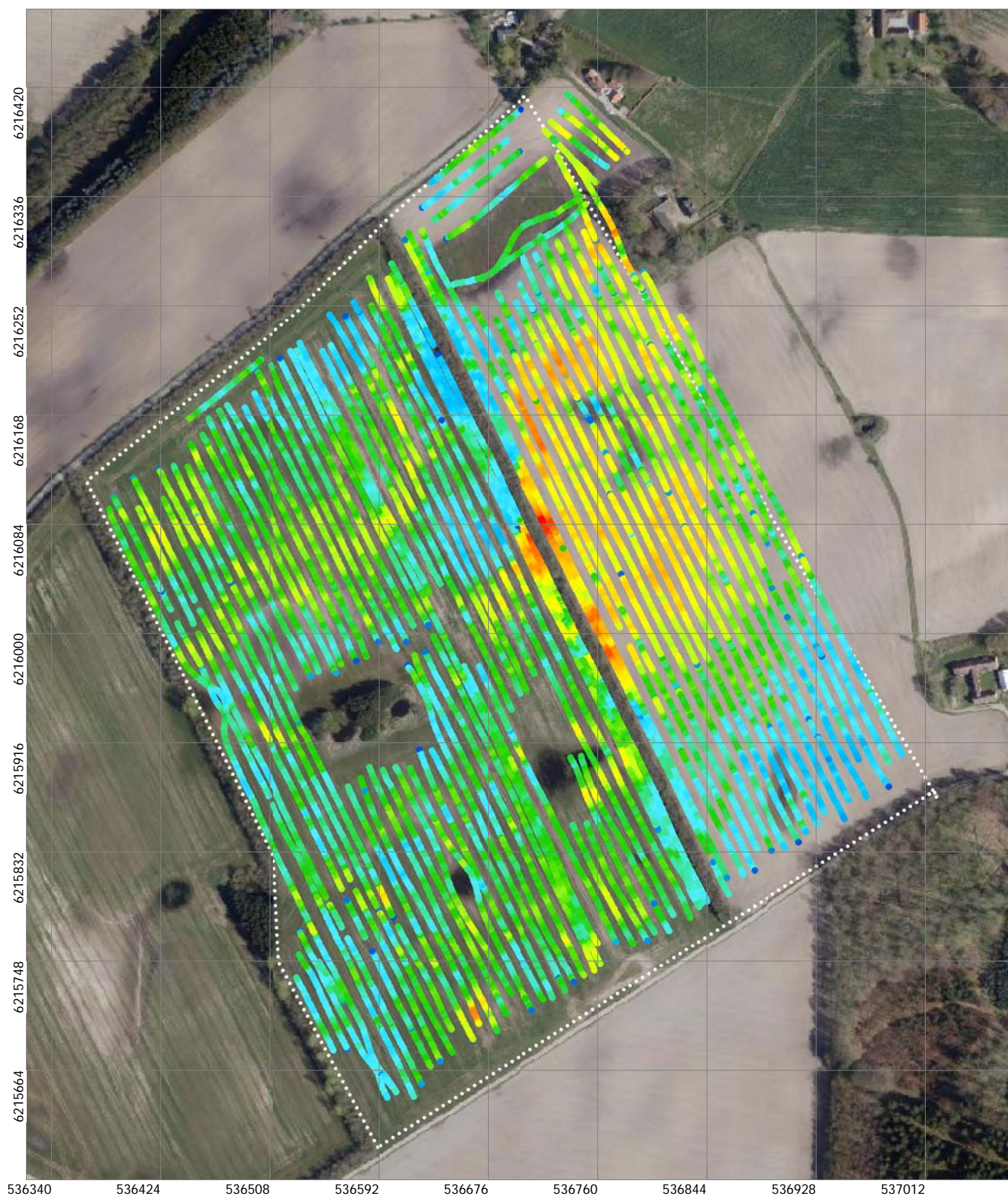




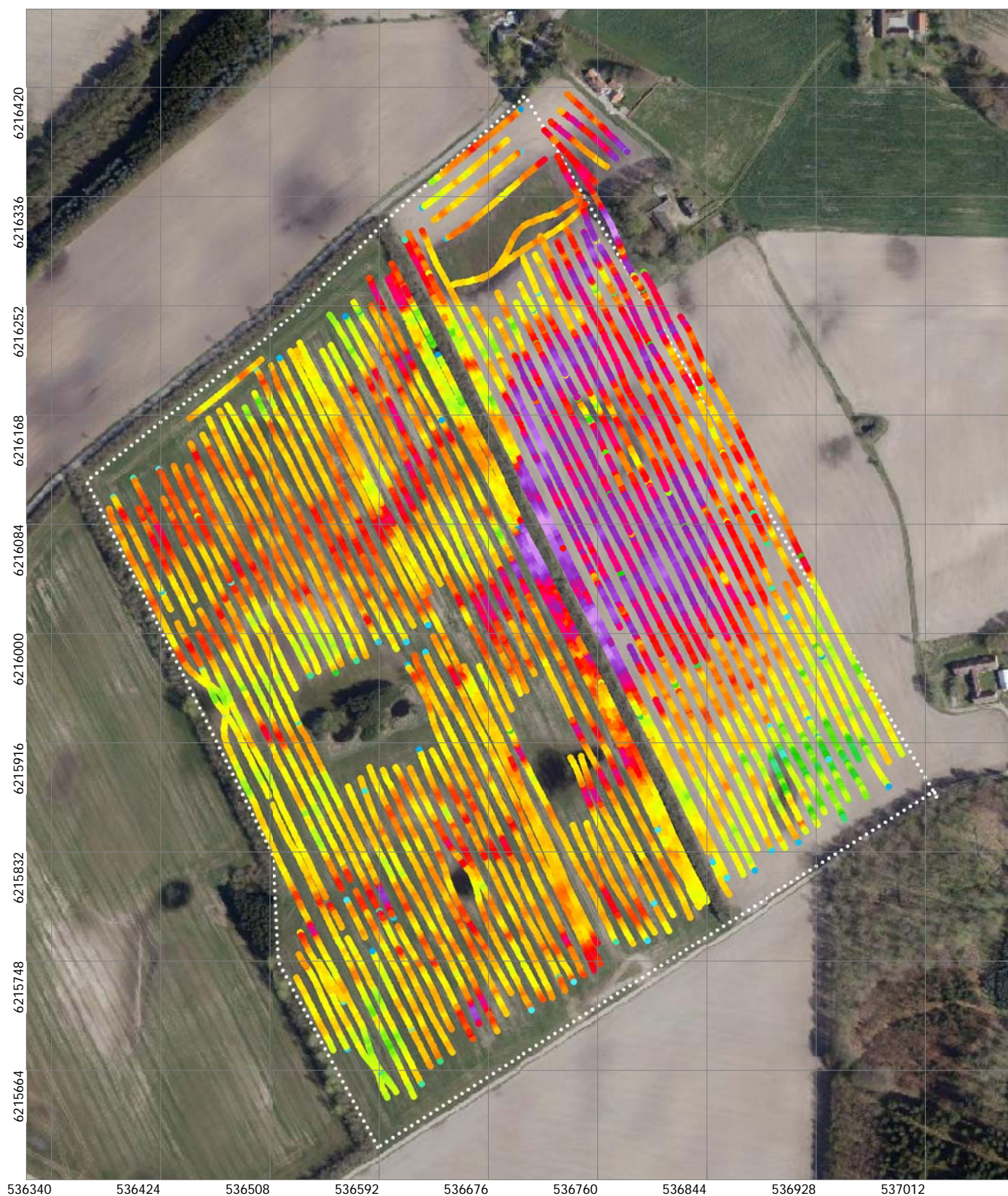










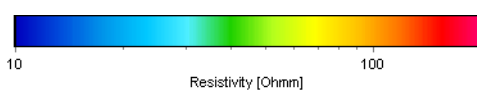
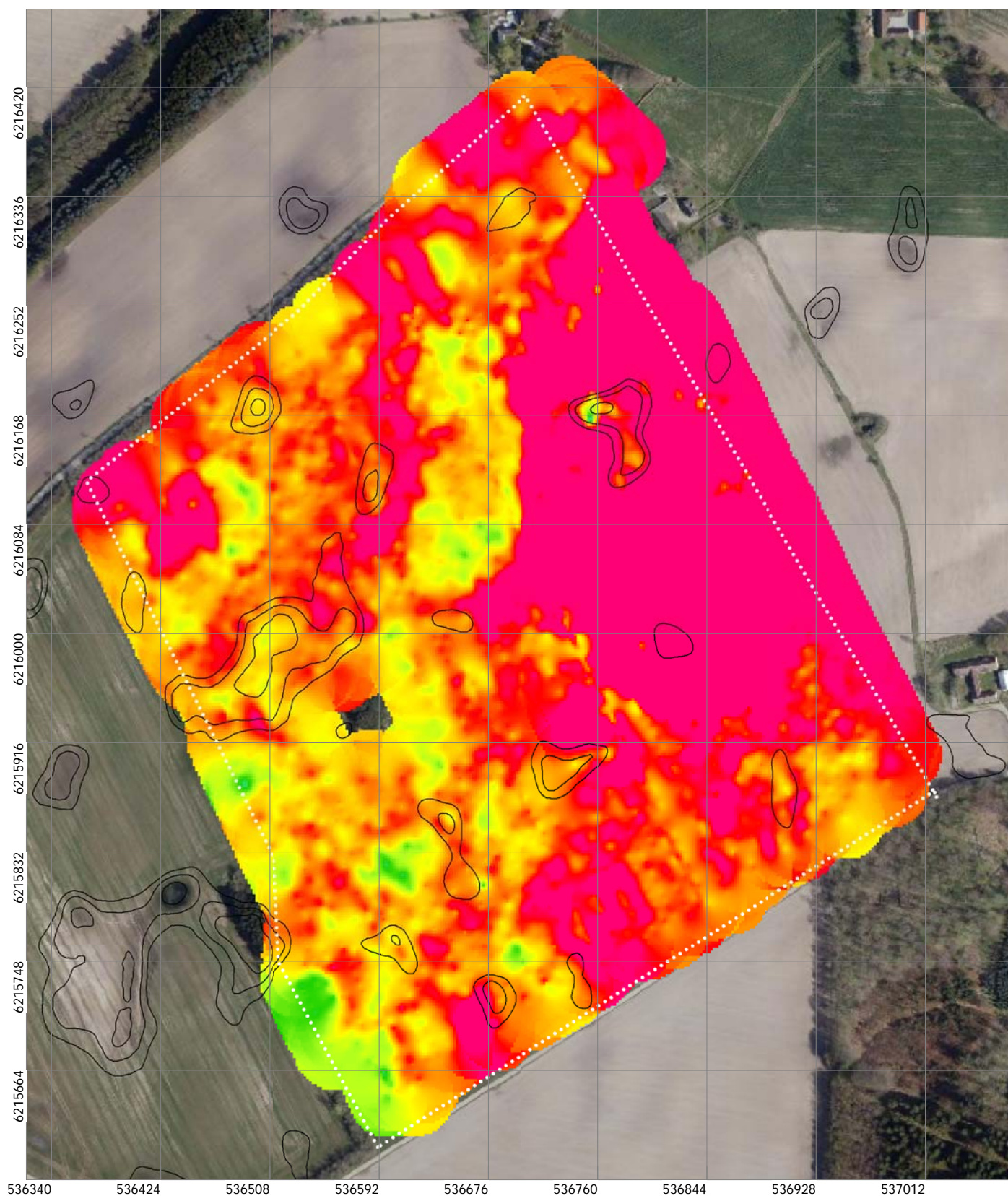




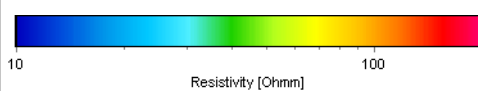
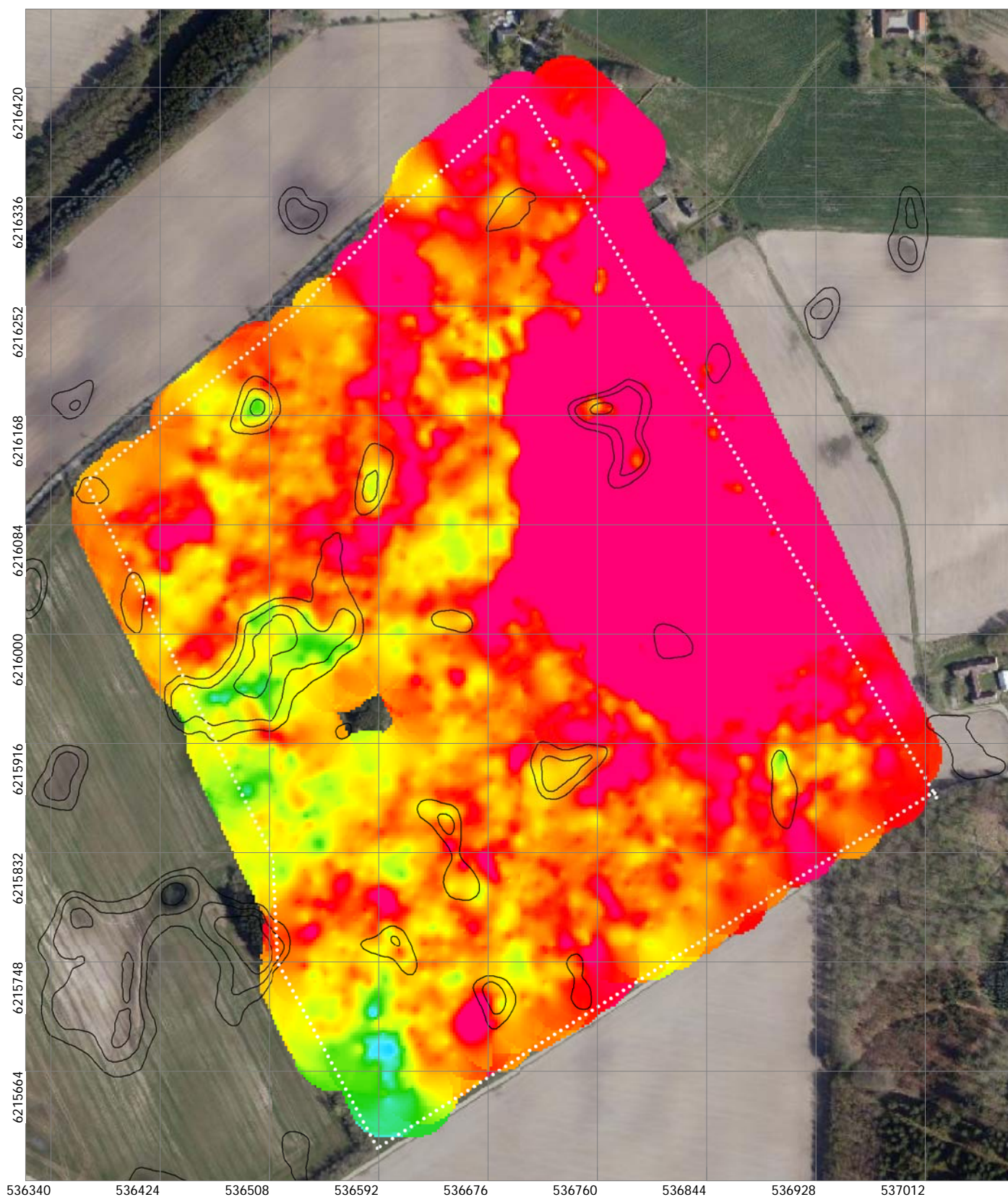
## 6.2 Mean Resistivity maps

In the following mean-resistivity maps are shown. Mean-resistivity maps are produced with 0.5 m intervals from a depth of 0-2 m and 1 m intervals from 2-5 m depth. From 5 m depth, the shown mean-resistivity maps are based on the tTEM results. The mean-resistivity maps are in 5 m slices from 5-30 m depth and 10 m slices from 30 to 50 m depth. In the calculation of the mean-resistivity maps the standard DOI limit is used as the cutting line, and model information below this limit is not included. Local lows in the terrain has been superimposed on the mean-resistivity maps as black contoured circles. The survey area is highlighted with a white polygon.

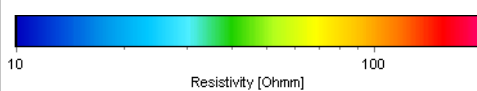
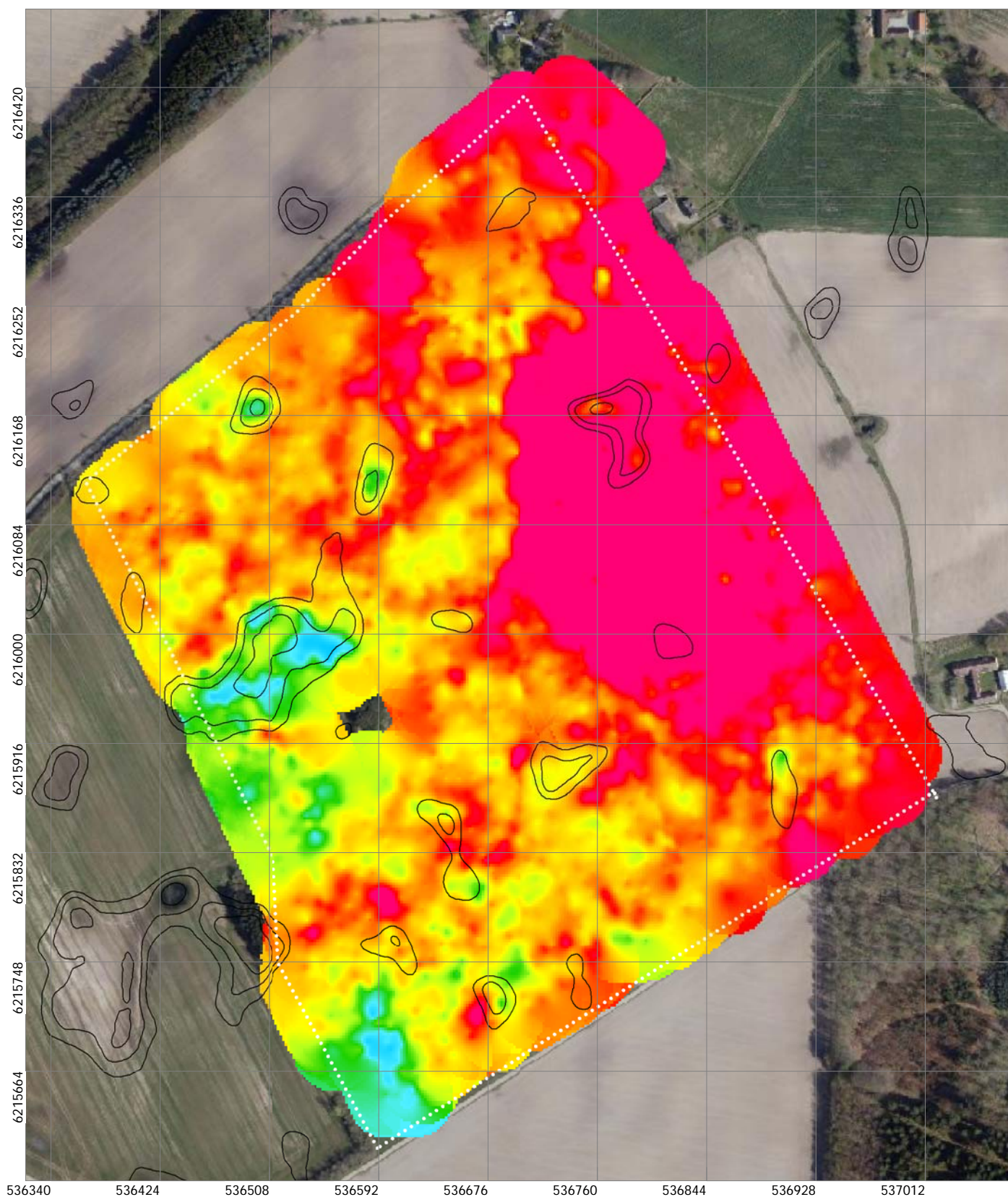




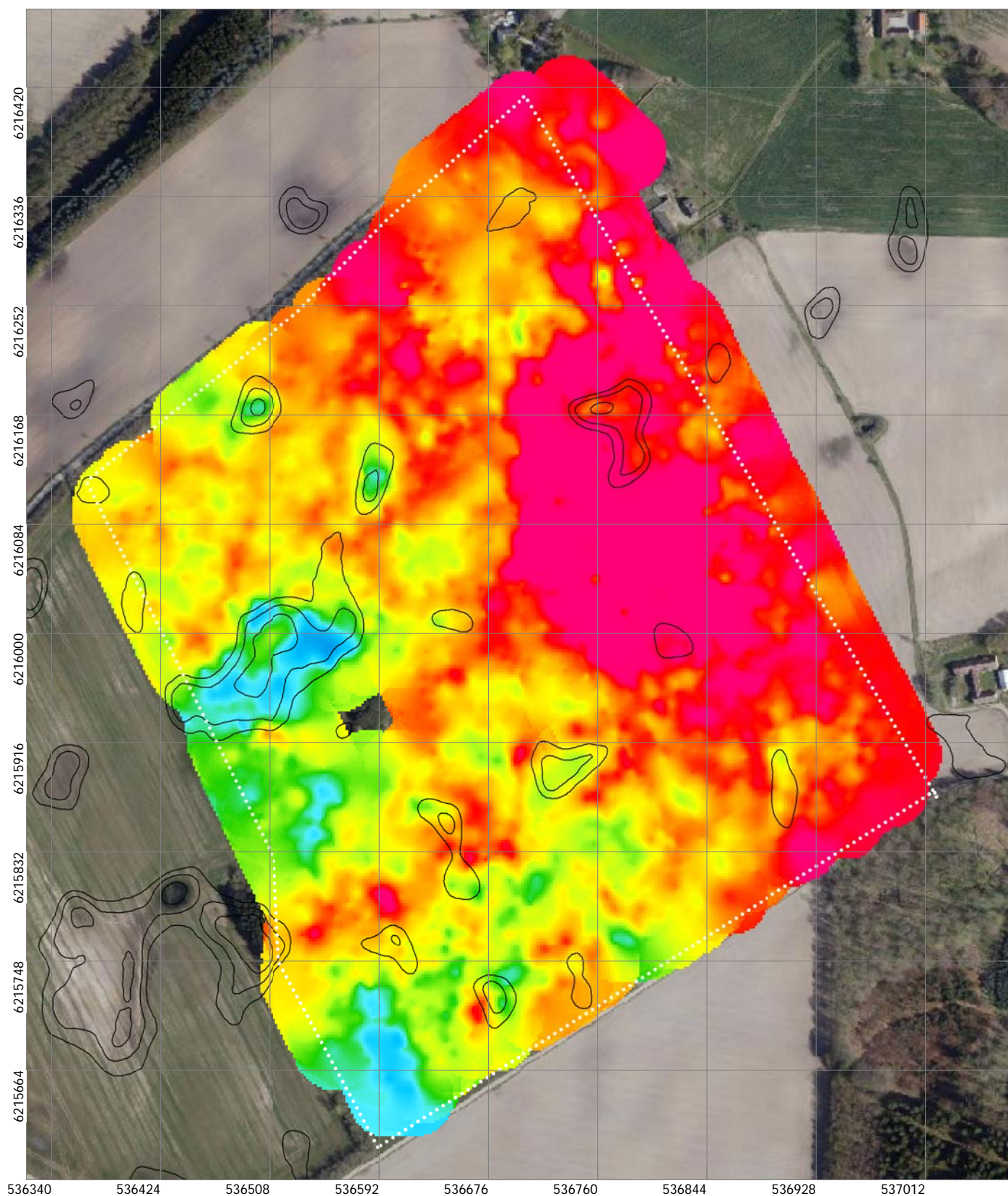








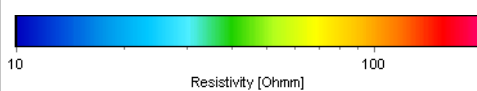




HydroGeophysics Group  
AARHUS UNIVERSITY

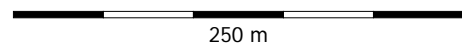


## GCM Salten 2017

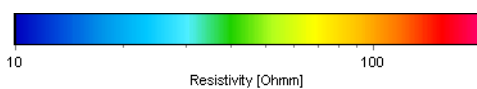
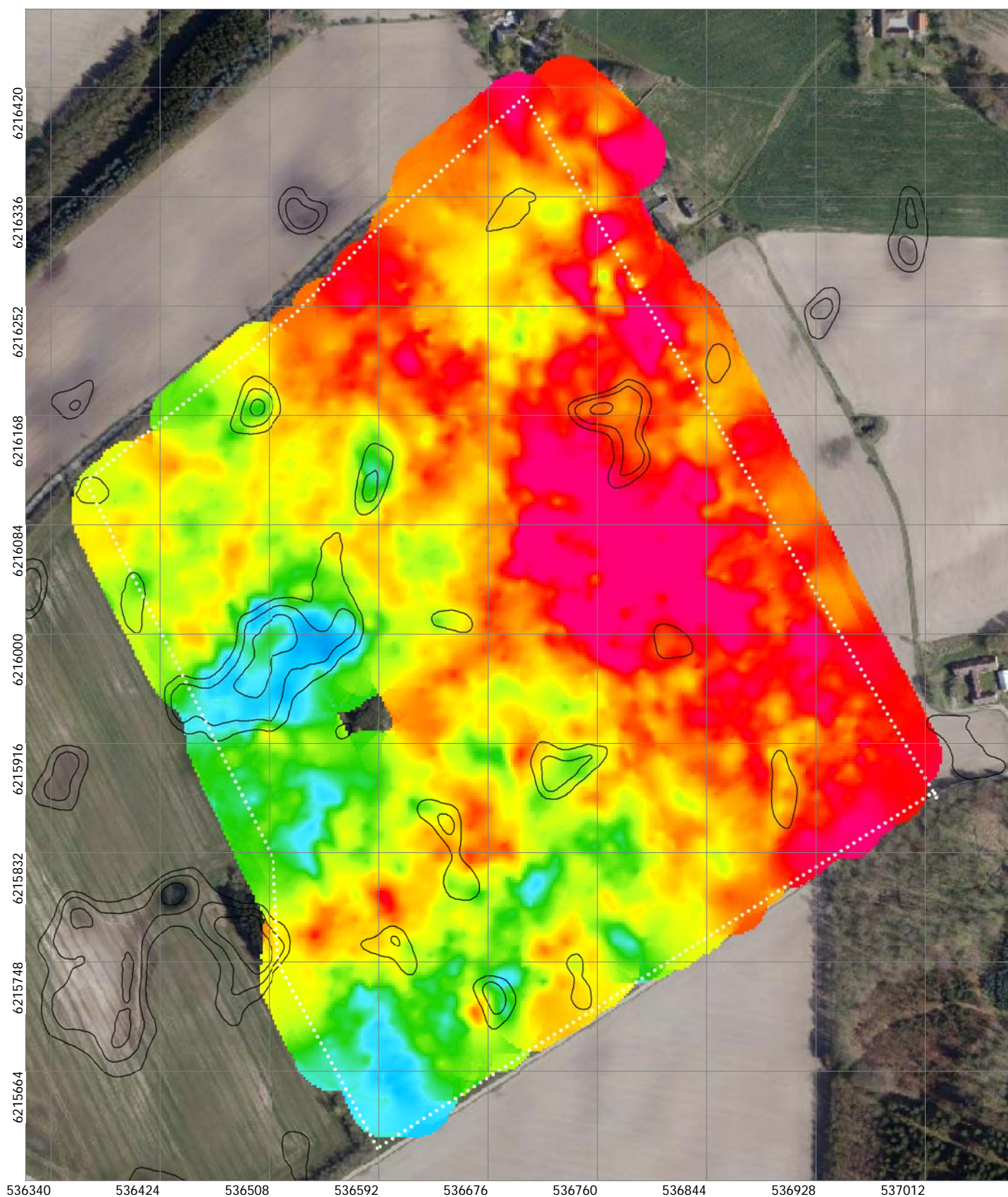


Mean-resistivity, Depth 1.5 m - 2.0 m (ohm-m)  
SCI Smooth Model - Kriging Search Radius 30 m

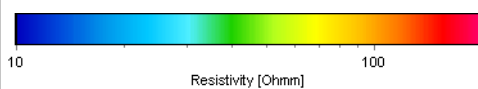
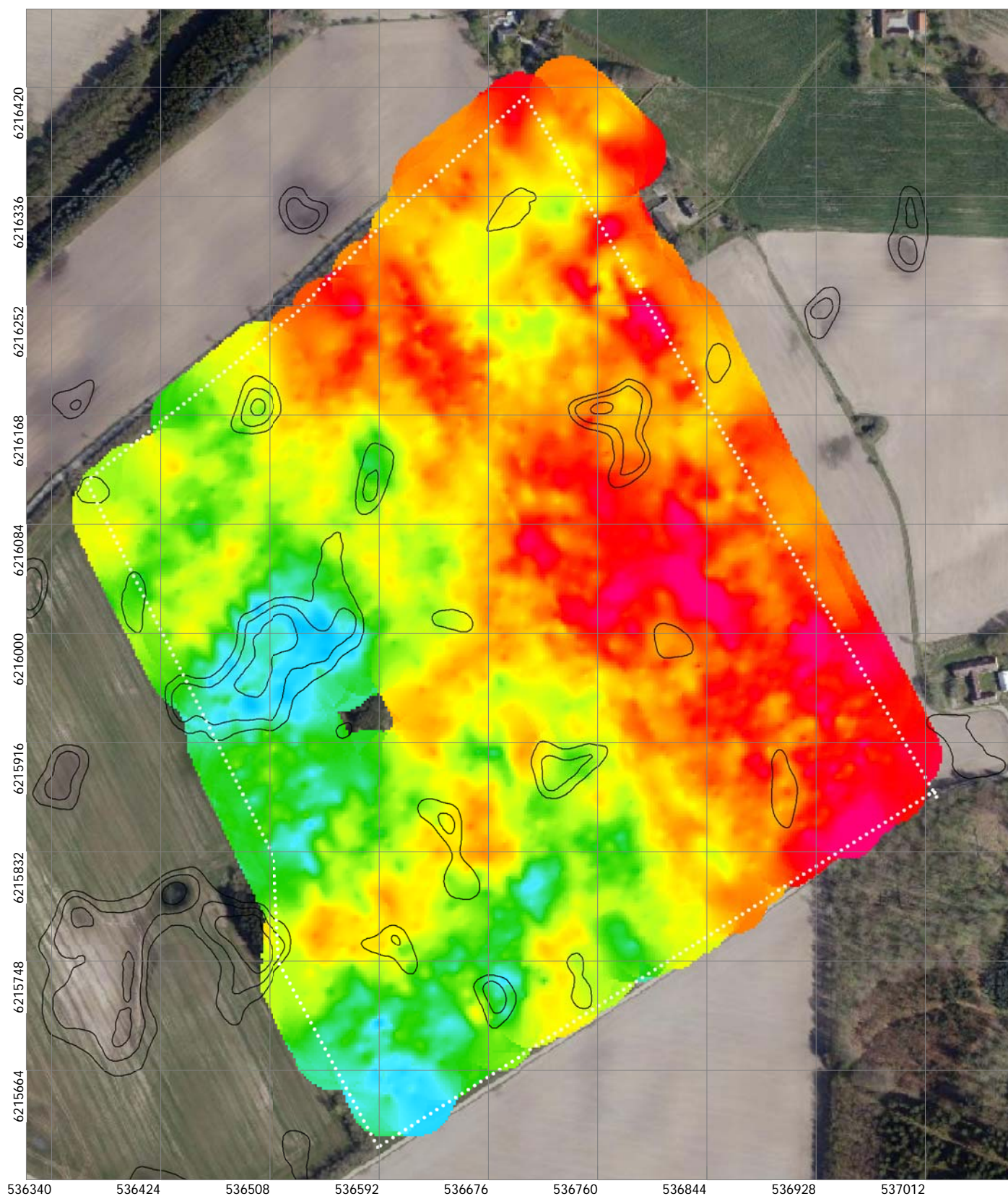
UTM 32N WGS84



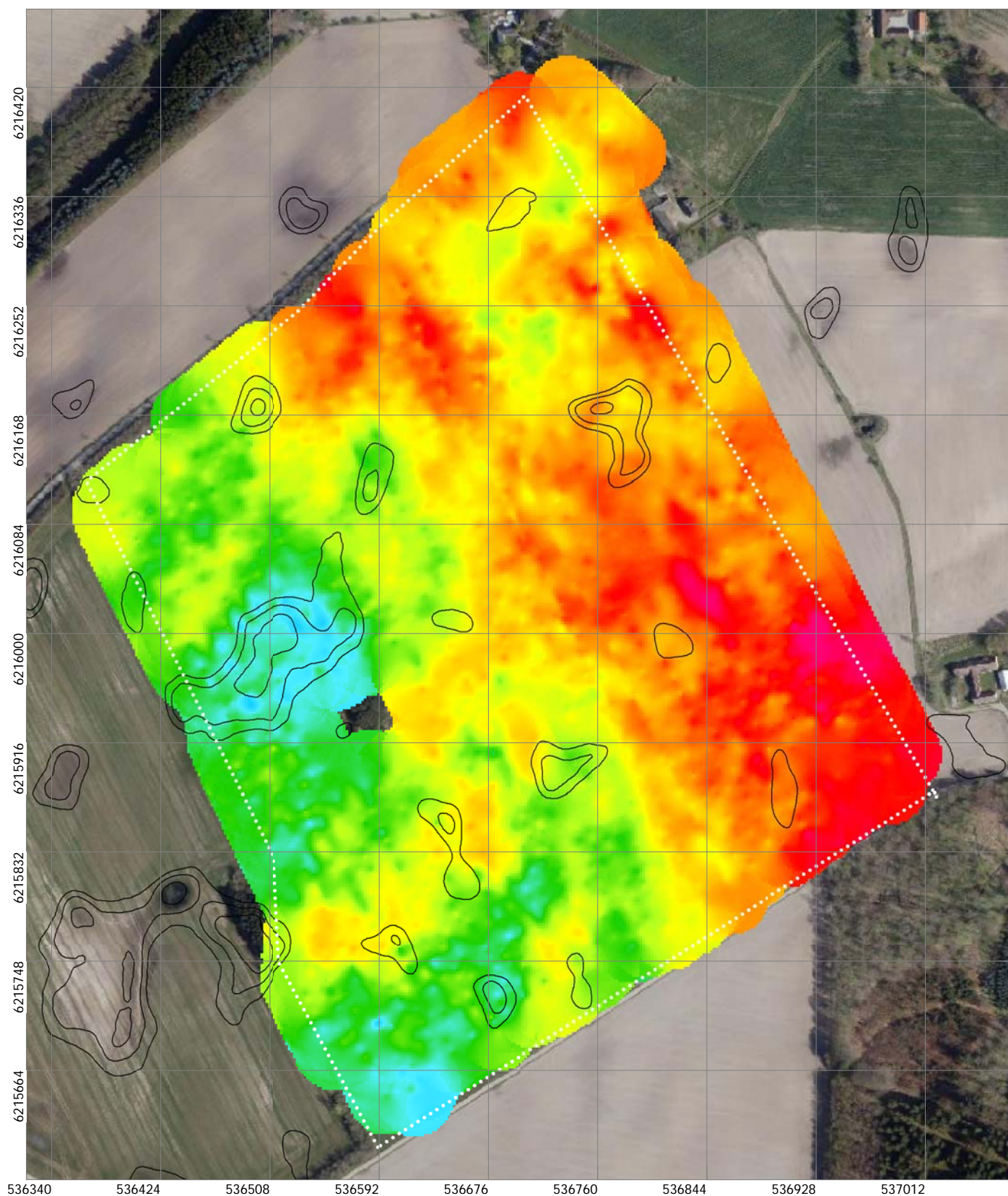








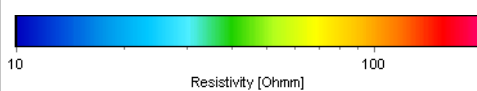




HydroGeophysics Group  
AARHUS UNIVERSITY

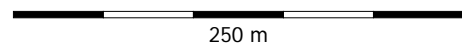


## GCM Salten 2017



Mean-resistivity, Depth 4.0 m - 5.0 m (ohm-m)  
SCI Smooth Model - Kriging Search Radius 30 m

UTM 32N WGS84



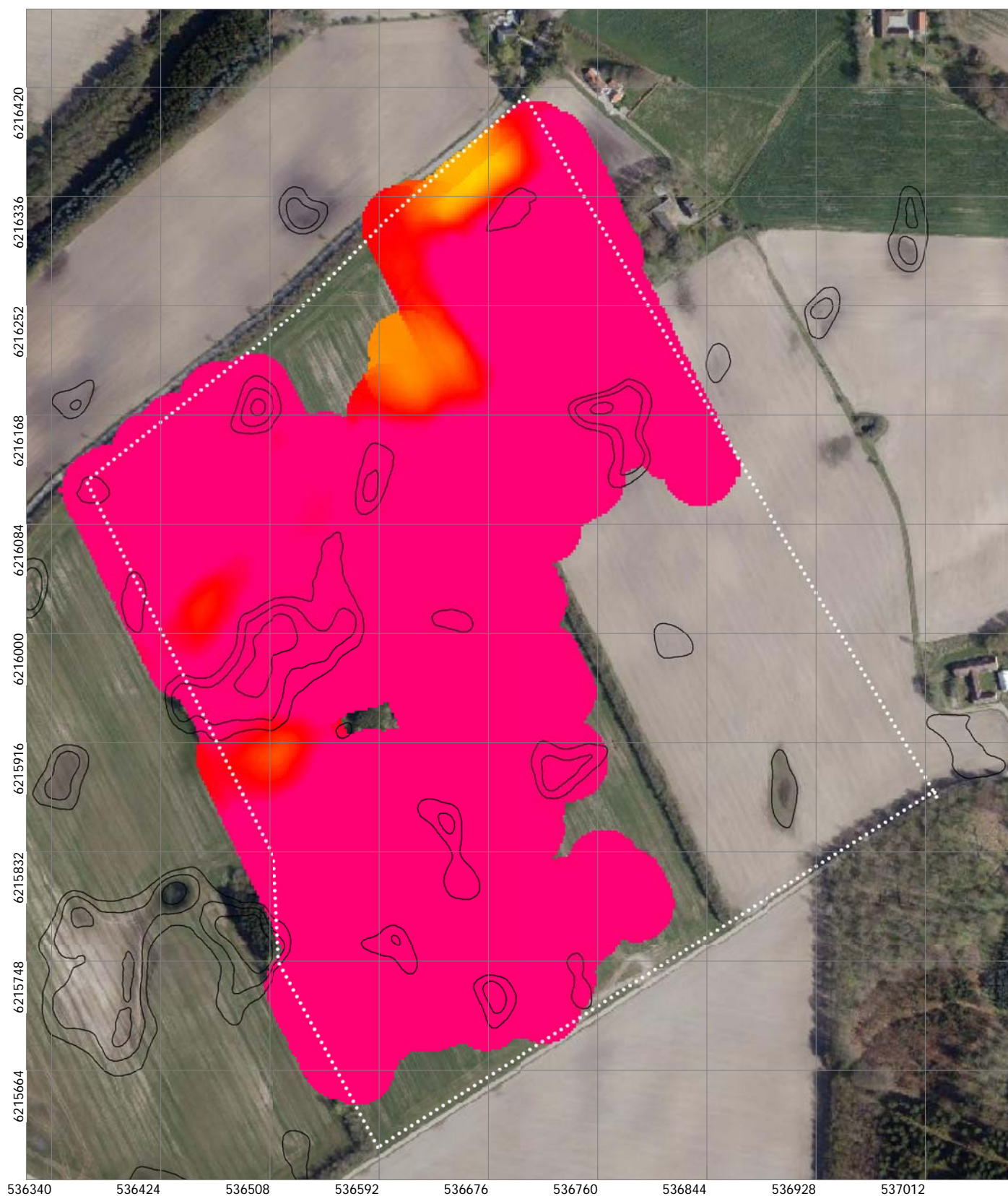




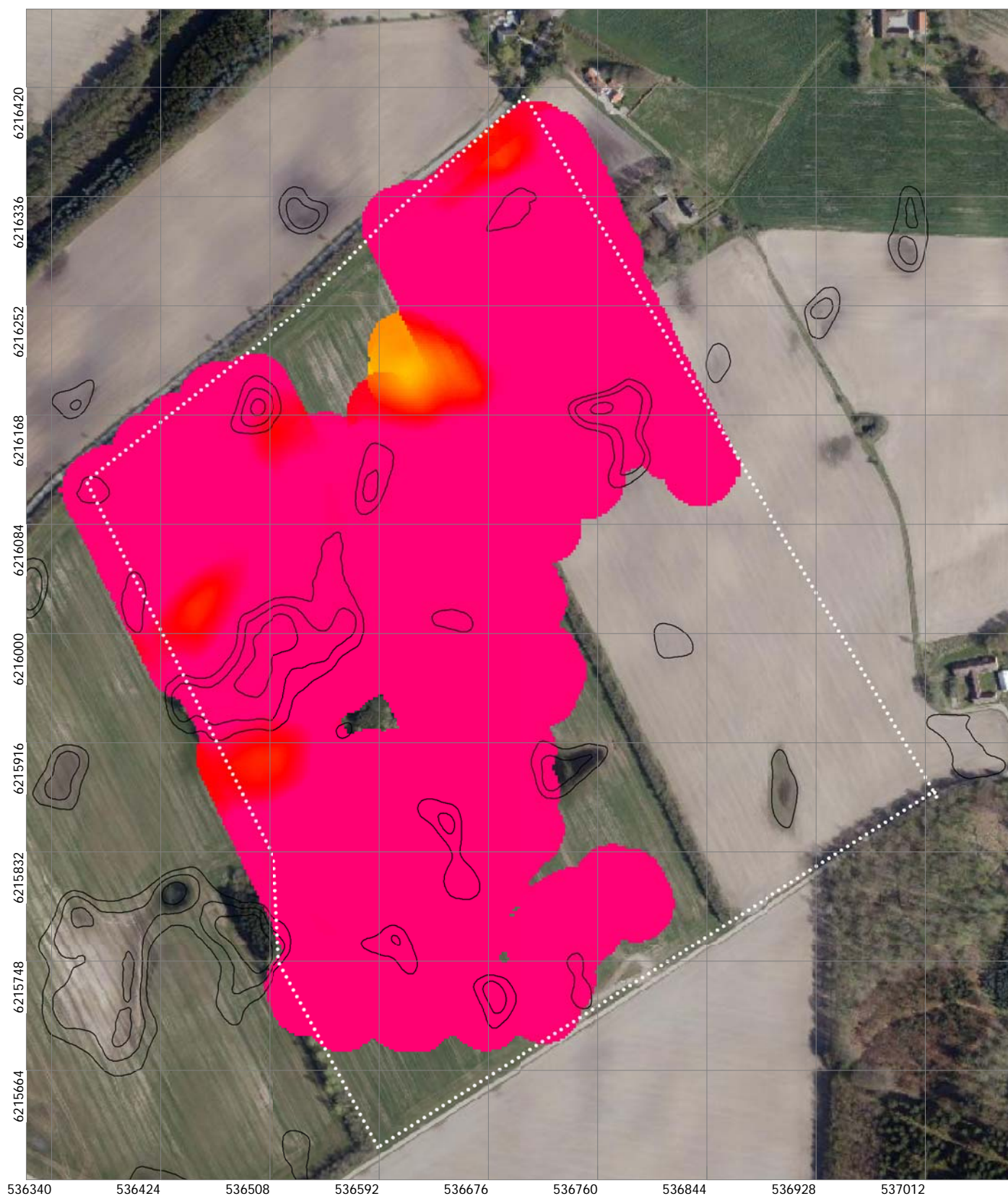


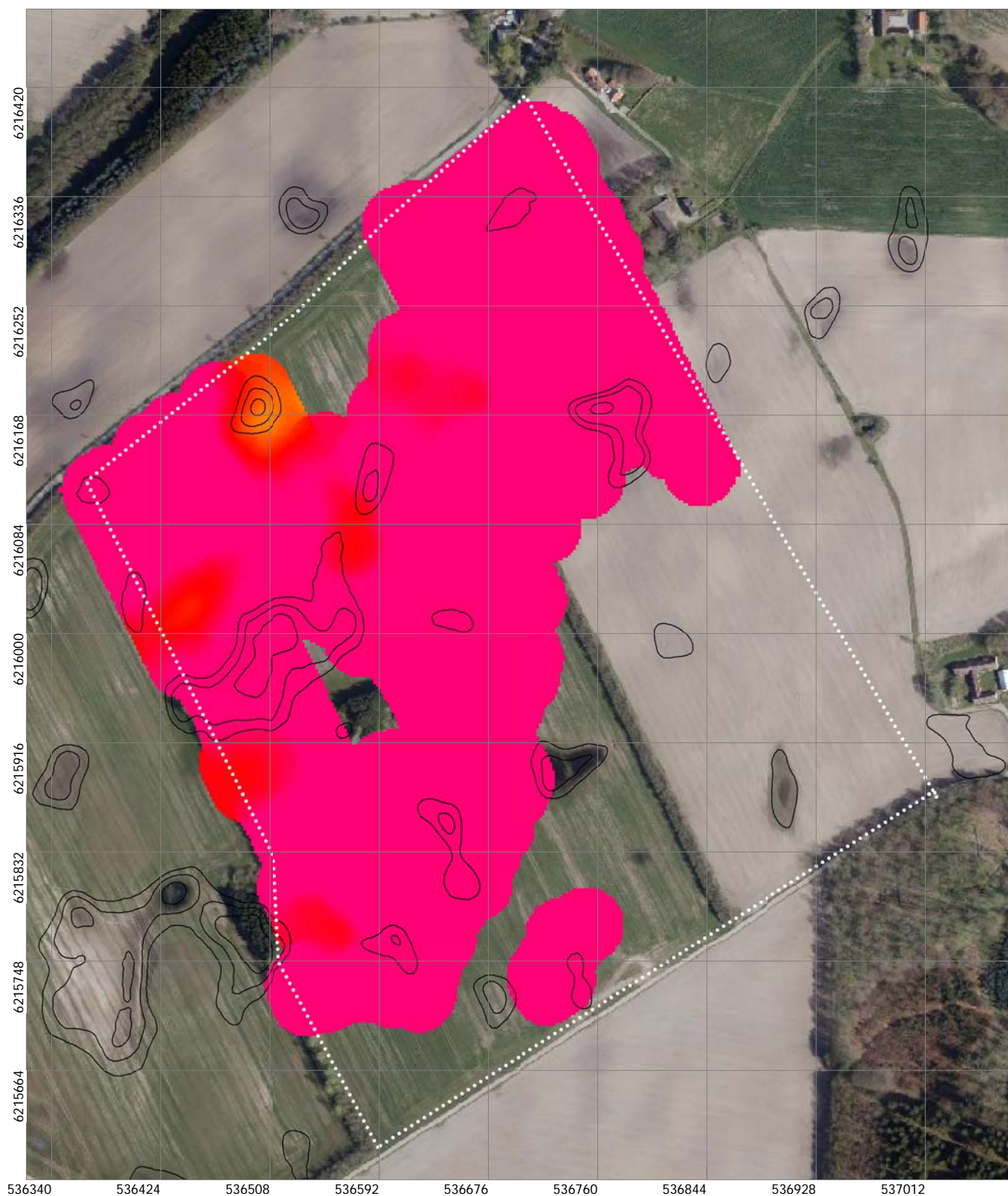














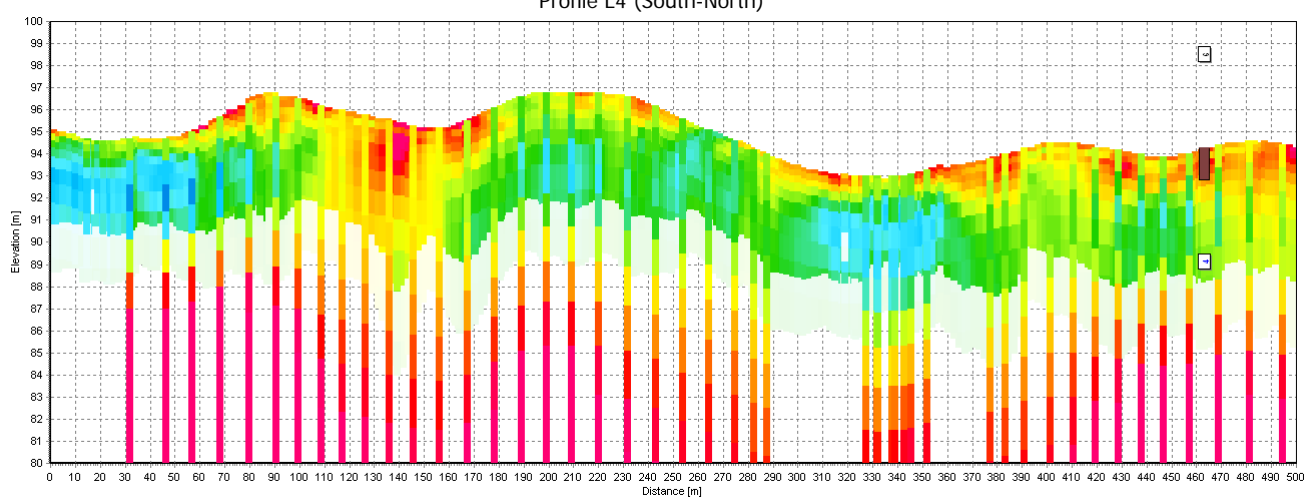


### 6.3 Profiles

In the profiles the smooth inversion results are shown as model bars. The colors below the standard DOI limit are faded. GCM and tTEM results are shown as model bars. GCM with 2 m distance between the models, and 10 m distance between the models for the tTEM results. The tTEM results are shown on top of the GCM. Superimposed on both are the boreholes. For a detailed description of the borehole lithology we refer the reader to the paper “Notat vedr. profilundersøgelser ved Løvenholt by GPS Agro/Casper Szilas”. The borehole number is written on top of each borehole. The number displayed in the bottom of the borehole is the distance between the profile and the borehole.



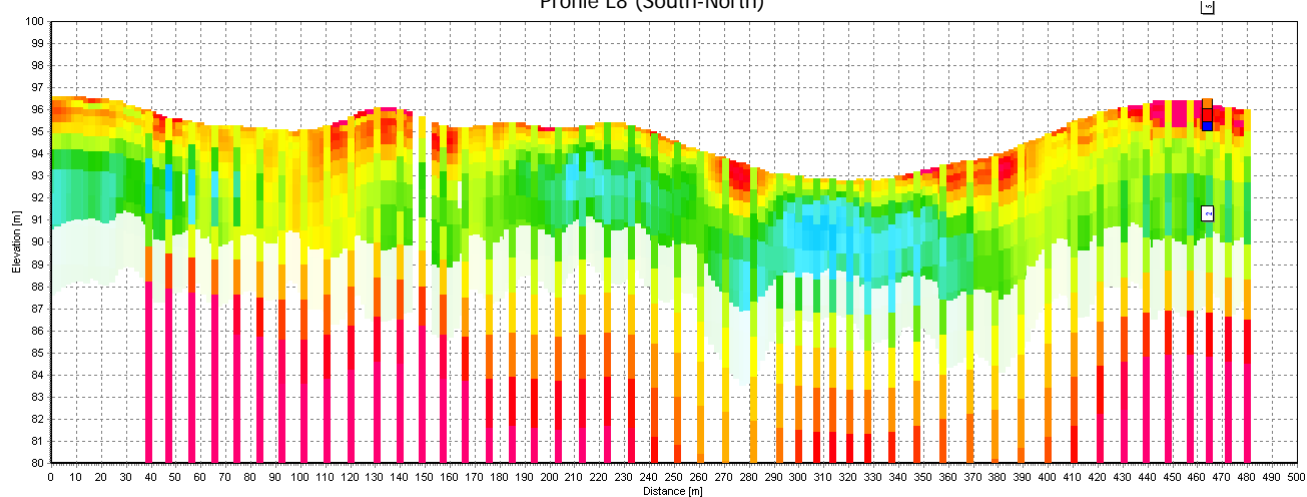
Profile L4 (South-North)







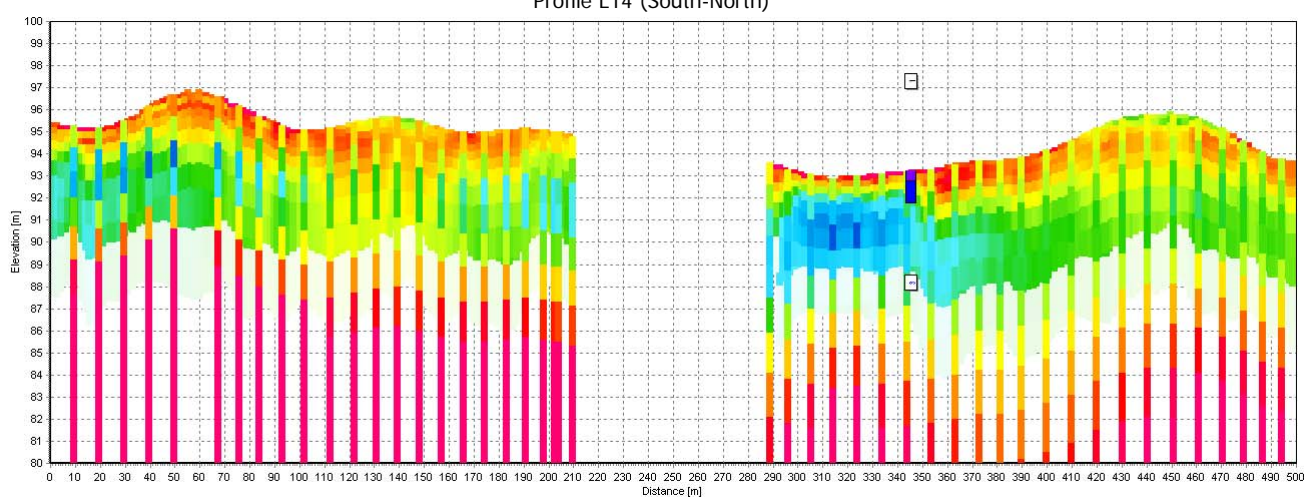
Profile L8 (South-North)







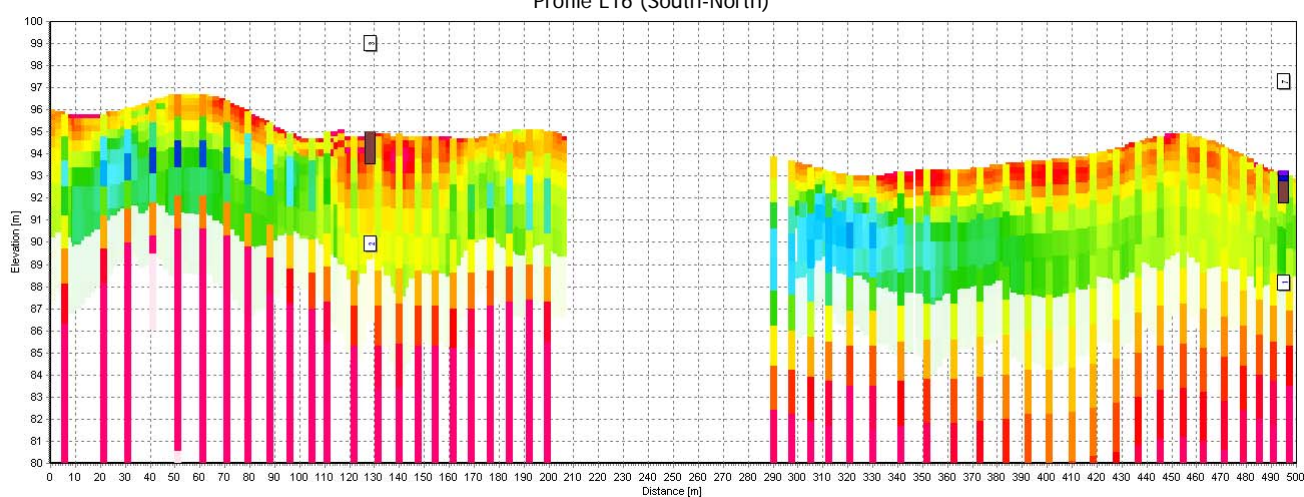
Profile L14 (South-North)







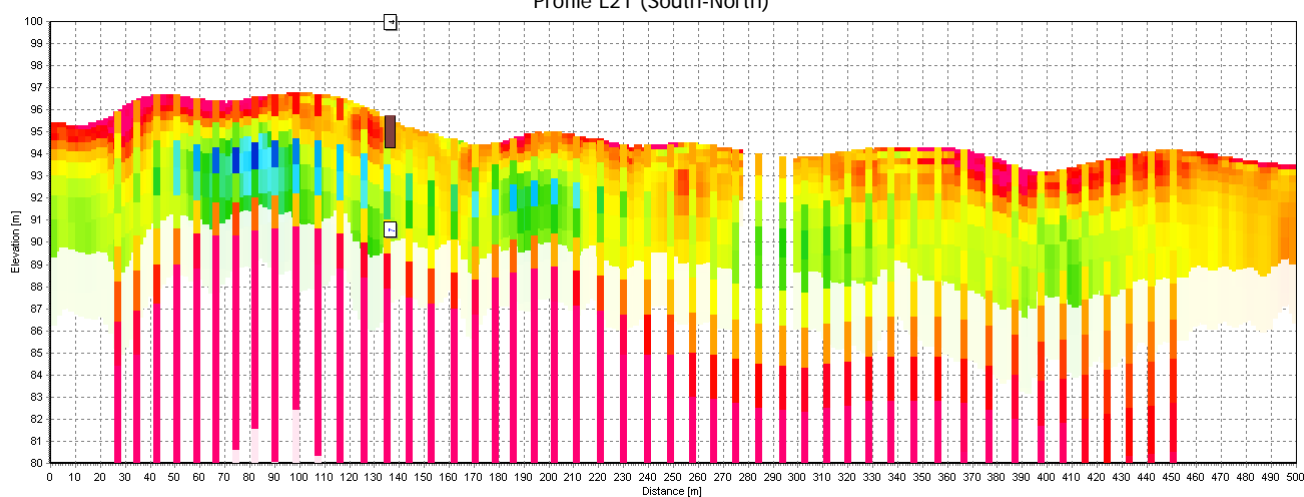
Profile L16 (South-North)







Profile L21 (South-North)







Profile L25 (South-North)

